Journal of Solid Mechanics Vol. 12, No. 1 (2020) pp. 165-174
DOI: 10.22034/jsm.2019.1867106.1430

A New Three-Dimensional Sector Element for Circular Curved Structures Analysis

H.E. Khiouani *, L. Belounar, M. Nabil Houhou

NMISSI Laboratory, Biskra University, BP145 Biskra 07000, Algeria

Received 15 November 2019; accepted 14 January 2020

ABSTRACT

In this research paper, the formulation of a new three-dimensional sector element based on the strain approach is presented for plate bending problems and linear static analysis of circular structures. The proposed element has the three essential external degrees of freedom (U_r, V_θ and W) at each of the eight corner nodes. The displacements field of the present element is based on assumed functions for the different strains satisfying the compatibility equations. The effectiveness of the present element is applied through several tests related to plate bending problems and linear static analysis of circular structures. The results of the developed element have been compared with analytical and other numerical solutions available in the literature. The obtained results show the excellent performances and precision of the present element. It is found that the new three-dimensional sector element is more accurate and efficient than the three-dimensional classical element based on displacement approach.

Keywords: Strain approach; Sector element; Field displacements; Circular structures; Plane elasticity.

1 INTRODUCTION

IN practice, engineers prefer to model their structures with simple finite elements, such as four-node quadrilaterals, three-node triangles, and eight-node 3D bricks. In recent years, the analysis of three-dimensional structures has made considerable progress in several domains. Many research works have been oriented towards three-dimensional elements using different approaches. For the classical displacement model, 3D low-order elements suffer from many numerical difficulties, while the use of 3D quadratic elements significantly improves the results accuracy but the computing cost becomes much higher. For these reasons, many researchers have been motivated to formulate simple and robust elements such as the 20-node solid element for shell analysis developed by Kim [1]. There are also other works set up to three-dimensional elements, for thick plates in bending [2-3]. Ayad [4] have proposed a 3D hexahedral finite element named SFR8 based on the space fiber rotation concept (SFR) where the computing cost is reduced compared to the classical quadratic 20-node hexahedral element. On the other hand, many 3D solid elements, in Cartesian coordinates, based on the strain approach have been developed for plate

*Corresponding author. Tel.: +213 663131789.
E-mail address: houssamkhiouani@gmail.com (H.E. Khiouani).

bending analysis [5-8]. These elements which contain three degrees of freedom (*U, V* and *W*) per node have been used with a modified elasticity matrix by introducing plane stress constants and a transverse shear corrective coefficient. The strain based element developed by Messai [8] has been extended for free vibration analysis. The nonlinear bending analysis of circular/annular graphene sheets has been used by Dastjerdi et al. [9-10]. All research works of references [9-11] are based on the nonlocal elasticity theory. The use of the strain-based approach plays a key role in the construction of robust and efficient finite elements. It is known that the strain approach allows having better precision on the displacements, strains and stresses where the displacements field is obtained by integrating assumed strains, contrary to the classical formulation where the strains are obtained by derivation of the displacements [12]. The advantages of formulating strain based finite elements have been reported by many researchers [13-16]. This approach allows to decouple the different components of the strain and to enrich the displacements field by terms of high order without the need to introduce internal nodes; this enables to solve locking problems [17]. The modeling of plane circular structures in polar coordinates whose behavior is membrane and based on the strain approach has been the subject of several research works [12, 18-19]. The first sector element developed by Sabir [18] contains two translations (U_r and V_θ) per node, whereas the sector elements formulated by Belarbi [12] and Bouzriba [19] posses the two translations and in-plane drilling rotation per node. To date, to the knowledge of the authors, no study was found in the literature for 3D sector elements based on the strain approach. This has motivated the authors to formulate a new strain based brick sector element.

In the present study, an eight-node 3D sector element based on the strain approach has been presented for static analysis of circular structures. This element named SBS3D (Strain Based Sector three-Dimensional) contains three translations (U_r, V_θ, W) at each of the eight corner nodes. The displacements field of this element has been formulated using the strain based approach and satisfy the compatibility equations. This element is evaluated and compared with analytical and other numerical solutions through several tests which confirmed the high performance of the current element.

2 FORMULATION OF THE SBS3D ELEMENT

The present element SBS3D is formulated using the displacements field of the strain-based 3D eight-node hexahedral element given in reference [6]. The displacement functions of this element in terms of Cartesian coordinates *x, y, z* are given as follows [6]:

$$\begin{aligned}
U &= a_1 + a_4 y + a_6 z + a_7 x + a_8 xy + a_9 xz + a_{10} xyz - 0.5a_{12} y^2 + 0.5a_{14} y^2 z - 0.5a_{16} z^2 \\
&\quad - 0.5a_{18} yz^2 + 0.5a_{19} y + 0.5a_{20} yz - 0.5a_{22} yz + 0.5a_{23} z + 0.5a_{24} yz \\
V &= a_2 - a_4 x - a_5 z - 0.5a_8 x^2 + 0.5a_{10} x^2 z + a_{11} y + a_{12} xy + a_{13} yz + a_{14} xyz - 0.5a_{17} z^2 \\
&\quad - 0.5a_{18} yz^2 + 0.5a_{19} x + 0.5a_{20} xz + 0.5a_{21} z + 0.5a_{22} xz - 0.5a_{24} xz \\
W &= a_3 + a_5 y - a_6 x - 0.5a_9 x^2 - 0.5a_{10} x^2 y - 05a_{13} y^2 - 0.5a_{14} xy^2 + a_{15} z + a_{16} xz + a_{17} yz \\
&\quad + a_{18} xyz - 0.5a_{20} xy + 0.5a_{21} y + 0.5a_{22} xy + 0.5a_{23} x + 0.5a_{24} xy
\end{aligned} \tag{1}$$

Considering the 3D sector SBS3D element shown in Fig. 1, the formulation of the SBS3D element is obtained by converting the displacements field given of Eq.(1) to cylindrical coordinates *r, θ* and *z* by replacing *x* and *y* with *r* and *θ*, respectively, as:

$$\begin{aligned}
x &= r \\
y &= \theta
\end{aligned} \tag{2}$$

This procedure of transformation, from the Cartesian (*x, y, z*) to cylindrical (*r, θ, z*) coordinates has been used by many researchers [12, 20]. By substituting Eq. (2) into Eq. (1) we obtain the final displacements field U_r, V_θ and W, respectively, in the radial, circumferential and axial directions as:

$$\begin{aligned}
U_r &= a_1 + a_4 \theta + a_6 z + a_7 r + a_8 r\theta + a_9 rz + a_{10} r\theta z - 0.5a_{12} \theta^2 + 0.5a_{14} \theta^2 z - 0.5a_{16} z^2 \\
&\quad - 0.5a_{18} \theta z^2 + 0.5a_{19} \theta + 0.5a_{20} \theta z - 0.5a_{22} \theta z + 0.5a_{23} z + 0.5a_{24} \theta z
\end{aligned} \tag{3}$$

$$V_\theta = a_2 - a_4 r - a_5 z - 0.5a_8 r^2 + 0.5a_{10} r^2 z + a_{11}\theta + a_{12} r\theta + a_{13}\theta z + a_{14} r\theta z - 0.5a_{17} z^2$$
$$- 0.5a_{18}\theta z^2 + 0.5a_{19} r + 0.5a_{20} rz + 0.5a_{21} z + 0.5a_{22} rz - 0.5a_{24} rz$$
$$W = a_3 + a_5\theta - a_6 r - 0.5a_9 r^2 - 0.5a_{10} r^2\theta - 05a_{13}\theta^2 - 0.5a_{14} r\theta^2 + a_{15} z + a_{16} rz + a_{17}\theta z$$
$$+ a_{18} r\theta z - 0.5a_{20} r\theta + 0.5a_{21}\theta + 0.5a_{22} r\theta + 0.5a_{23} r + 0.5a_{24} r\theta$$

The SBS3D element with three degrees of freedom (U_r, V_θ and W) at each of the eight corner nodes is shown in Fig.1, where r_1 and r_2 are the internal and external radius, respectively.

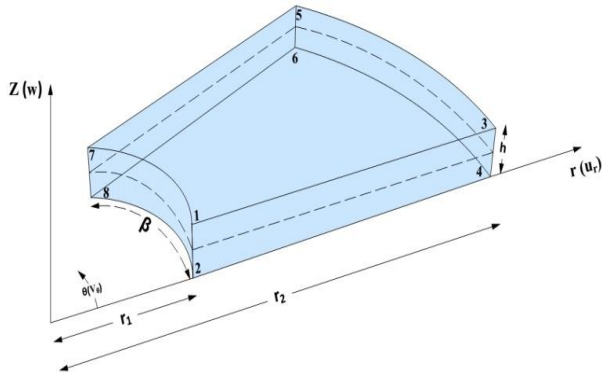

Fig.1
Brick sector element SBS3D with U_r, V_θ and W translations at each of the eight nodes.

In cylindrical coordinates r, θ and z, the strain-displacement relationships and the compatibility equations are, respectively, expressed as follows:

$$\varepsilon_r = \frac{\partial u_r}{\partial r}, \qquad \gamma_{r\theta} = \frac{\partial u_r}{r\partial\theta} + \frac{\partial v_\theta}{\partial r} - \frac{v_\theta}{r}$$
$$\varepsilon_\theta = \frac{u_r}{r} + \frac{\partial v_\theta}{r\partial\theta}, \qquad \gamma_{\theta z} = \frac{\partial w}{r\partial\theta} + \frac{\partial v_\theta}{\partial z} \tag{4}$$
$$\varepsilon_z = \frac{\partial w}{\partial z}, \qquad \gamma_{rz} = \frac{\partial u_r}{\partial z} + \frac{\partial w}{\partial r}$$

$$\frac{\partial^2\varepsilon_r}{\partial z^2} + \frac{\partial^2\varepsilon_z}{\partial r^2} = \frac{\partial^2\gamma_{rz}}{\partial r\partial z}$$
$$\frac{\partial^2\varepsilon_\theta}{\partial z^2} + \frac{1}{r^2}\frac{\partial^2\varepsilon_z}{\partial\theta^2} + \frac{1}{r}\frac{\partial\varepsilon_z}{\partial r} = \frac{1}{r}\frac{\partial}{\partial z}\left[\frac{\partial\gamma_{\theta z}}{\partial\theta} + \gamma_{rz}\right]$$
$$\frac{1}{r}\frac{\partial^2\varepsilon_r}{\partial\theta^2} + \frac{1}{r}\frac{\partial}{\partial r}\left[r^2\frac{\partial\varepsilon_\theta}{\partial r}\right] - \frac{\partial\varepsilon_r}{\partial r} = \frac{1}{r}\frac{\partial^2(r\gamma_{r\theta})}{\partial r\partial\theta}$$
$$\frac{\partial^2\gamma_{r\theta}}{\partial z^2} - r\frac{\partial^2}{\partial r\partial z}\left[\frac{\gamma_{\theta z}}{r}\right] - \frac{1}{r}\frac{\partial^2\gamma_{rz}}{\partial\theta\partial z} = -2\frac{\partial^2}{\partial r\partial\theta}\left[\frac{\varepsilon_z}{r}\right] \tag{5}$$
$$\frac{\partial}{\partial r}\left(\frac{1}{r}\frac{\partial(r\gamma_{\theta z})}{\partial r}\right) - \frac{1}{r^2}\left(\frac{\partial^2(r^2\gamma_{r\theta})}{\partial r\partial z}\right) - \frac{\partial^2}{\partial r\partial\theta}\left(\frac{\gamma_{rz}}{r}\right) = -\frac{2}{r}\frac{\partial^2\varepsilon_r}{\partial\theta\partial z}$$
$$\frac{\partial^2\gamma_{rz}}{\partial\theta^2} - \frac{\partial^2(r\gamma_{\theta z})}{\partial r\partial\theta} - \frac{\partial^2(r\gamma_{r\theta})}{\partial\theta\partial z} = 2r\frac{\partial}{\partial z}\left[\varepsilon_r - \frac{\partial(r\varepsilon_\theta)}{\partial r}\right]$$

where U_r, V_θ and W are the displacements in the r, θ and z directions, respectively, while ε_r, ε_θ and ε_z are the direct strains, and $\gamma_{r\theta}$, $\gamma_{\theta z}$ and γ_{rz} are the shear strains.

The strains field can be obtained by substituting Eq. (3) into Eq. (4):

$$
\begin{aligned}
\varepsilon_r &= a_7 + a_8\theta + a_9 z + a_{10} z\,\theta \\
\varepsilon_\theta &= \frac{1}{r}a_1 + \frac{\theta}{r}a_4 + \frac{z}{r}a_5 + a_7 + a_8\theta + a_9 z + a_{10} z\,\theta + \frac{1}{r}a_{11} + \left(1 - \frac{\theta^2}{2r}\right)a_{12} + \frac{z}{r}a_{13} + \left(z + \frac{z\,\theta^2}{2r}\right)a_{14} \\
&\quad - \frac{1}{2r}z^2 a_{16} - \frac{1}{2r}z^2\theta a_{18} + \frac{\theta}{2r}a_{19} + \frac{z\,\theta}{2r}a_{20} - \frac{z\,\theta}{2r}a_{22} + \frac{z}{2r}a_{23} + \frac{z\,\theta}{2r}a_{24} \\
\varepsilon_z &= a_{15} + a_{16}\theta + a_{17} z + a_{18} z\,\theta \\
\gamma_{r\theta} &= -\frac{1}{r}a_1 + \frac{1}{r}a_4 + \frac{z}{r}a_5 + \left(1 - \frac{1}{2}r\right)a_8 + \left(z + \frac{zr}{2}\right)a_{10} - \frac{\theta}{r}a_{11} - \frac{\theta}{r}a_{12} - \frac{z\,\theta}{r}a_{13} + \frac{z\,\theta}{r}a_{14} \\
&\quad + \frac{z^2}{2r}a_{17} - \frac{z^2}{2r}a_{18} + \frac{1}{2r}a_{19} + \frac{z}{2r}a_{20} - \frac{z}{2r}a_{21} - \frac{z}{2r}a_{22} + \frac{z}{2r}a_{24} \\
\gamma_{\theta z} &= \left(\frac{1}{r} - 1\right)a_5 + \left(\frac{1}{2} - \frac{1}{2r}\right)a_{10} + \left(\theta - \frac{\theta}{r}\right)a_{13} + (r\theta - \theta)a_{14} + \left(\frac{z}{r} - z\right)a_{17} + (z - zr)a_{18} \\
&\quad + \left(\frac{1}{2r} - \frac{1}{2}\right)a_{20} + \left(\frac{1}{2} + \frac{1}{2r}\right)a_{21} + \left(\frac{1}{2r} + \frac{1}{2}\right)a_{22} + \left(\frac{1}{2} - \frac{1}{2}r\right)a_{24} \\
\theta &= a_{23} + a_{24}\theta
\end{aligned}
\tag{6}
$$

The obtained strain functions given by Eq. (6) for the SBS3D element satisfy the compatibility (Eq. (5)). The displacements and the strain functions given in Eqs. (3) and (6) are, respectively, given in matrix form:

$$
\begin{Bmatrix} U_r \\ V_\theta \\ W \end{Bmatrix} = [P]\{\mathrm{A}\} \tag{7}
$$

$$
\begin{Bmatrix} \varepsilon_r \\ \varepsilon_\theta \\ \varepsilon_z \\ \gamma_{r\theta} \\ \gamma_{\theta z} \\ \gamma_{rz} \end{Bmatrix} = [Q]\{\mathrm{A}\} \tag{8}
$$

where:

$$
[P] = \begin{bmatrix}
1 & 0 & 0 & \theta & 0 & z & r & r\theta & rz & r\theta z & 0 & -\frac{1}{2}\theta^2 & 0 & \frac{1}{2}\theta^2 z & 0 & -\frac{1}{2}z^2 & 0 & -\frac{\theta z^2}{2} & \frac{\theta}{2} & \frac{\theta z}{2} & 0 & -\frac{\theta z}{2} & \frac{z}{2} & \frac{\theta z}{2} \\
0 & 1 & 0 & -r & -z & 0 & 0 & -\frac{1}{2}r^2 & 0 & -\frac{1}{2}r^2 z & \theta & r\theta & \theta z & r\theta z & 0 & 0 & -\frac{1}{2}z^2 & -\frac{1}{2}rz^2 & -\frac{1}{2}r & \frac{1}{2}rz & \frac{1}{2}z & \frac{1}{2}rz & 0 & -\frac{1}{2}rz \\
0 & 0 & 1 & 0 & \theta & -r & 0 & 0 & -\frac{r^2}{2} & -\frac{r^2\theta}{2} & 0 & 0 & -\frac{\theta^2}{2} & -\frac{r\theta^2}{2} & z & rz & \theta z & r\theta z & 0 & -\frac{r\theta}{2} & \frac{\theta}{2} & \frac{r\theta}{2} & \frac{r}{2} & \frac{r\theta}{2}
\end{bmatrix}
$$

$$
[Q] = \begin{bmatrix}
0 & 0 & 0 & 0 & 0 & 0 & 1 & \theta & z & z\theta & 0 & 0 & 0 & 0 & 0 & 0 & 0 & 0 & 0 & 0 & 0 & 0 & 0 & 0 \\
\frac{1}{r} & 0 & 0 & \frac{\theta}{r} & 0 & \frac{z}{r} & 1 & \theta & z & z\theta & \frac{1}{r} & \left(1-\theta^2\right) & \frac{z}{r} & \left(z+z\theta^2\right) & 0 & -\frac{z^2}{2r} & 0 & -\frac{z^2\theta}{2r} & \frac{\theta}{2r} & \frac{z\theta}{2r} & 0 & -\frac{z\theta}{2r} & \frac{z}{2r} & \frac{z\theta}{2r} \\
0 & 0 & 0 & 0 & 0 & 0 & 0 & 0 & 0 & 0 & 0 & 0 & 0 & 0 & 1 & r & \theta & r\theta & 0 & 0 & 0 & 0 & 0 & 0 \\
0 & -\frac{1}{r} & 0 & \frac{1}{r} & \frac{z}{r} & 0 & 0 & 1-\frac{1}{2}r & 0 & \frac{1}{2}z(r+2) & -\frac{\theta}{r} & -\frac{\theta}{r} & -\frac{z\theta}{r} & \frac{z\theta}{r} & 0 & 0 & \frac{z^2}{2r} & -\frac{z^2}{2r} & \frac{1}{2r} & \frac{z}{2r} & -\frac{z}{2r} & -\frac{z}{2r} & 0 & \frac{z}{2r} \\
0 & 0 & 0 & 0 & \left(\frac{1}{r}-r\right) & 0 & 0 & 0 & 0 & \frac{r}{2}(r-1) & 0 & 0 & \frac{\theta}{r}(r-1) & \theta(r-1) & 0 & 0 & -\frac{z}{r}(r-1) & -z(r-1) & 0 & \frac{r}{2}-\frac{1}{2} & \frac{1}{2r}(r+1) & \frac{r}{2}+\frac{1}{2} & 0 & \frac{1}{2}-\frac{r}{2} \\
0 & 0 & 0 & 0 & 0 & 0 & 0 & 0 & 0 & 0 & 0 & 0 & 0 & 0 & 0 & 0 & 0 & 0 & 0 & 0 & 0 & 0 & 1 & \theta
\end{bmatrix}
$$

$$
\{\mathrm{A}\} = [a_1, a_2, a_3, a_4, a_5, a_6, a_7, a_8 \ldots, a_{24}]^T
$$

The stiffness matrix for the 3D sector element is obtained by the usual expression of the finite element method as:

$$\left[K^{e}\right]=\int\left[B\right]^{T}\left[D\right]\left[B\right]dV \tag{9}$$

$$\left[K^{e}\right]=\left[C^{-1}\right]^{T}\left[\iiint\left[Q(r,\theta,z)\right]^{T}\left[D\right]\left[Q(r,\theta,z)\right]rdrd\theta dz\right]\left[C^{-1}\right]=\left[C^{-1}\right]^{T}\left[K_{0}\right]\left[C^{-1}\right] \tag{10}$$

where:

$$\left[B\right]=\left[Q\right]\left[C^{-1}\right] \tag{11}$$

where $[C]$ and $[D]$ which are respectively the transformation and the elasticity matrices are given in the appendix.

$$\iiint drd\theta dz=\int_{-1}^{+1}\int_{-1}^{+1}\int_{-1}^{+1}\det\left[J\right]d\varsigma d\eta\, d\zeta \tag{12}$$

$$\left[K^{e}\right]=\left[C^{-1}\right]^{T}\left[\int_{-1}^{+1}\int_{-1}^{+1}\int_{-1}^{+1}r\left[Q\right]^{T}\left[D\right]\left[Q\right]\det\left[J\right]d\varsigma d\eta\, d\zeta\right]\left[C^{-1}\right] \tag{13}$$

3 NUMERICAL VALIDATIONS

The purpose of this part is to show the interest of the strain model for the calculation of structures with circular contours. To evaluate the performance of the present element SBS3D, several numerical examples are investigated.

3.1 Thick cylinder subjected to uniform internal pressure

The first problem considered is that of a thick cylinder subjected to a uniform internal pressure where the geometrical and mechanical characteristics are presented in Fig. 2. For reasons of symmetry, only a quarter of the cylinder is considered for the idealization. Fig. 3 shows the results obtained for the radial deflection at the middle point E (r = 30 *mm*), which illustrates the high precision obtained by the sector element SBS3D. For example, for a mesh size 2×2 elements the error accounts is equal to 2.35 % of the analytical solution.

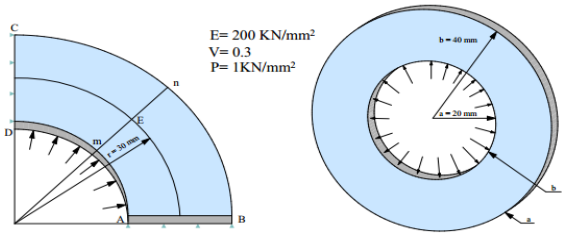

Fig.2
Thick cylinder under internal uniform pressure.

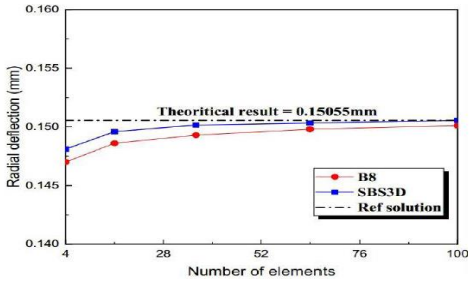

Fig.3
Convergence of radial deflection (U_r) at E(r=30 *mm*).

Moreover, the results obtained for the radial and tangential stresses at (r= 30mm) shown in Fig. 4, are satisfactory and converge to the theoretical solution as the number of elements is increased.

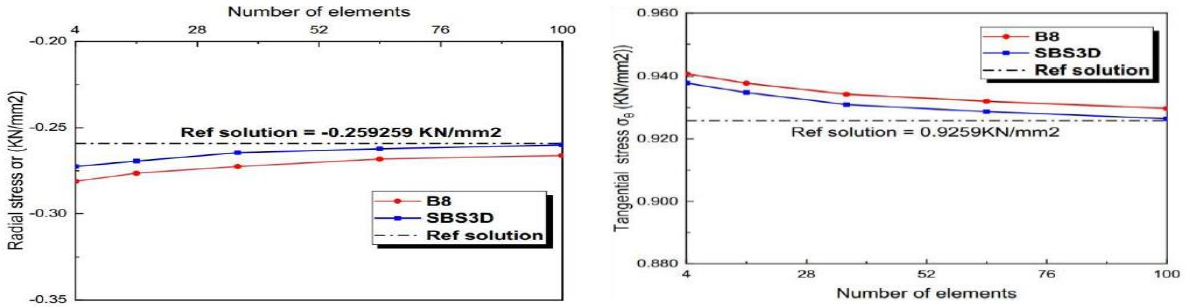

Fig.4
Convergence of radial ((σ_r) and tangential (σ_θ) stress at $E(r = 30\ mm)$.

Fig. 5 shows the variation of U_r across a section (m, n). The values obtained from the developed sector element SBS3D are compared to the analytical solution.

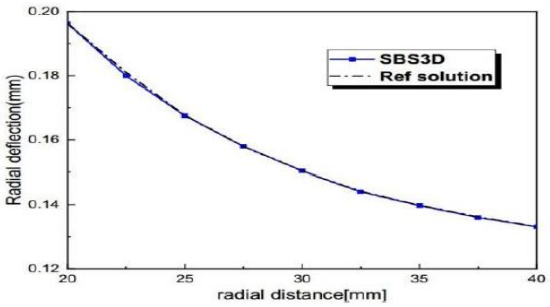

Fig.5
Variation of radial deflection (U_r) across cylinder wall.

The results obtained converge to the theoretical solution of the considered problem, and confirm the good performance of the sector element SBS3D compared to the classical element based on the displacement approach B8.

3.2 Annular plate under a lateral point load

The second example treated by Olson and Lindberg [21] is the annular plate clamped along the inner edge ($r_1 = b$) and loaded by a lateral force (z-direction) at the outer edge ($r_2 = a$) (see Fig. 6). Due to symmetry, only one half of the plate is analyzed, and the analytical solution of Timoshenko and Woinowsky-Kieger [22] is used for a= 1.0, b= 1.5 and v= 0.3. The results for the lateral displacement (w) under the concentrated force presented in Table 1., and Fig. 7 show the high rate of convergence to the analytical results for the sector element SBS3D.

According to the results obtained (see Table 1), it should be noted that when analyzing this problem with a (3 × 12) mesh for the two elements, the error is about 1.29% and 4.91% for Olson's element and present element, respectively. However, for (3 × 18) grid the present element presents a very good performance, where the error is reduced to 0.095%, and for Olson's element it is reduced to 0.61%. Fig. 7 shows that the lateral deflection for the present element along the inner edge converges rapidly to the exact solution when the mesh size is refined.

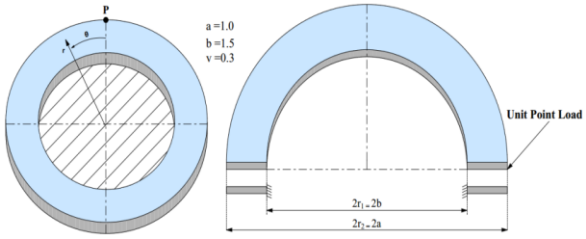

Fig.6
Annular plate subjected to a lateral point load.

Table 1
Lateral deflections under the applied point load.

Mesh	Olson's élément	SBS3D
1 × 6	0.050896	0.02707
2 × 8	0.051456	0.04204
2 × 12	0.051372	0.04562
3 × 12	0.051372	0.04823
3 × 18	0.051027	0.05067
Ref solution	0.0507180	

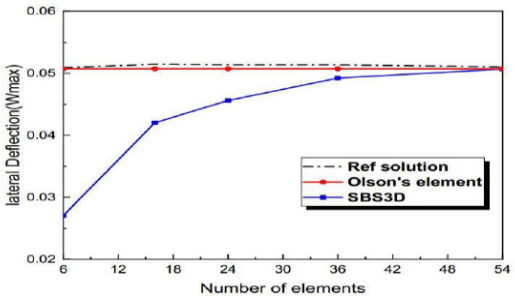

Fig.7
Convergence curve for the displacement *W* (Annular Plate).

3.3 Thick-walled cylinder subjected to internal pressure

This example of a thick-walled cylinder subjected to internal pressure, treated by Choi [23], is considered as plane strain problem. This test is used to study the locking phenomenon of elements and their behaviors related to nearly incompressible material. Due to symmetry, only a quarter of the cylinder is analyzed, physical and geometrical parameters are shown in Fig. 8. The value of Poisson's ratio is taken as 0.3, 0.49, 0.499 and 0.4999. The computed results for the radial deflection of the inner wall presented in Table 2., show that the developed element, restricted Poisson's locking effectively contrary to the other elements B8 and Q4 and its accuracy is quite high.

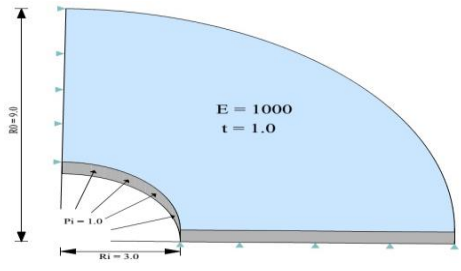

Fig.8
Thick walled cylinder subject to unit internal pressure.

Table 2
Normalized radial displacement at the inner wall of a thick cylinder in Fig. 8.

v	B8	Q4	SBS3D	Exact(10^{-3})
0.3	0.987	0.978	0.9909	4.5825
0.49	0.877	0.738	0.996	5.0399
0.499	0.796	0.224	0.997	5.0602
0.4999	0.532	0.028	0.997	5.0623

3.4 Bending of a curved bar by a force at the end

The semi-circular annular plate shown in Fig. 9 is subjected to two equilibrating shearing force applied at the upper end in the radial direction. The radial deflection results obtained are presented for a different number of ratios *b/a* = 3, 2, and 1.3. Due to symmetry, only half of the plate is analyzed. The results of radial deflection, as well as the stresses, can be compared with the analytical elasticity solution given by Timoshenko and Goodier [24] and the classical element based on the displacement approach B8.

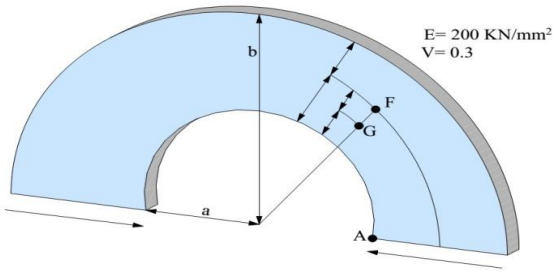

Fig.9
Annulus subjected to radial shear.

Figs. 10, 11 and 12 show the convergence for the radial deflection at point "A" for b/a = 3, 2 and 1.3, respectively. These curves are obtained when the same number of elements is used in the radial and circumferential directions. From these figures, it can be noted that the results given by SBS3D element converge rapidly to the analytical solution from a mesh of 4 × 4, and remain stable from a mesh of 8 × 8. Fig.13 shows the convergence of radial stresses at point "F" (see Fig. 9) in the case of b/a = 2. This element has been found to give better results for radial stress when a coarse mesh is used.

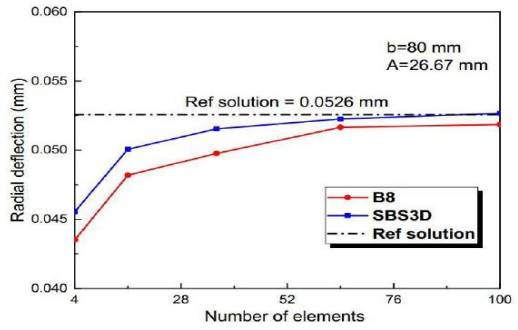

Fig.10
Convergence for the radial deflection (U_r) at point A for b/a=3.

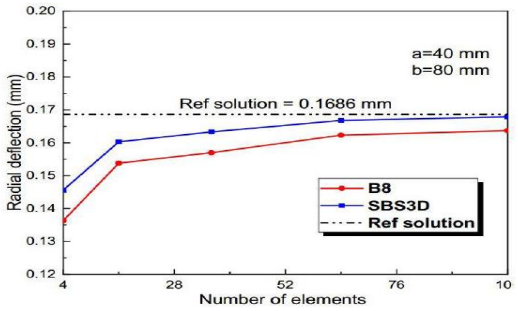

Fig.11
Convergence for the radial deflection (U_r) at point A for b/a=2.

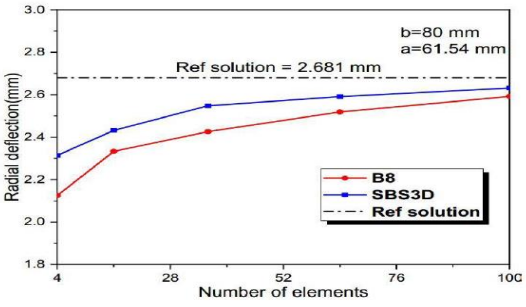

Fig.12
Convergence for the radial deflection (U_r) at point A for b/a=1.3.

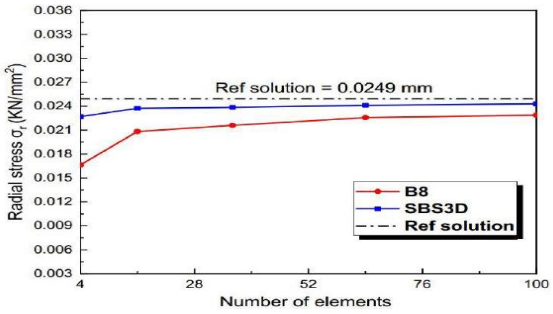

Fig.13
Convergence for the radial stress ($\bar{\sigma}_r$) at point F.

4 CONCLUSION

In this paper, a new three-dimensional sector element (SBS3D) based on the strain approach with eight nodes and three translations at each node is proposed for the analysis of annular thin plate bending and elasticity problems. A series of numerical examples have been studied to evaluate the effectiveness of the present element. The numerical results of this element are compared with reference and other numerical solutions. The SBS3D elements have shown good performance and rapid convergence to the theoretical solutions for all tests. In addition, it can be seen that the present element has eliminated the Poisson's locking contrary to the classical element B8 based on displacement approach.

APPENDIX

The transformation matrix [*C*] (24 × 24) for the SBS3D element is as follows:

$$[C]=\begin{bmatrix} P_1(r_1,\theta_1,z_1) \\ P_2(r_2,\theta_2,z_2) \\ P_3(r_3,\theta_3,z_3) \\ P_4(r_4,\theta_4,z_4) \\ P_5(r_5,\theta_5,z_5) \\ P_6(r_6,\theta_6,z_6) \\ P_7(r_7,\theta_7,z_7) \\ P_8(r_8,\theta_8,z_8) \end{bmatrix}$$

where the 3×24 matrix $[P_i]$ from Eq. (7) is given as follows:

$$[P(r_i,\theta_i,Z_i)]=$$

$$\begin{bmatrix} 1 & 0 & 0 & \theta_i & 0 & z_i & r_i & r_i\theta_i & r_iz_i & r_i\theta_iz_i & 0 & -\frac{1}{2}\theta_i^2 & 0 & \frac{1}{2}\theta_i^2 z_i & 0 & -\frac{1}{2}z_i^2 & 0 & -\frac{\theta_i z_i^2}{2} & \frac{\theta_i}{2} & \frac{\theta_i z_i}{2} & 0 & -\frac{\theta_i z_i}{2} & \frac{z_i}{2} & \frac{\theta_i z_i}{2} \\ 0 & 1 & 0 & -r_i & -z_i & 0 & 0 & -\frac{1}{2}r_i^2 & 0 & -\frac{1}{2}r_i^2 z_i & \theta_i & r_i\theta_i & \theta_i z_i & r_i\theta_i z_i & 0 & 0 & -\frac{1}{2}z_i^2 & -\frac{1}{2}r_i z_i^2 & -\frac{1}{2}r_i & \frac{1}{2}r_i z_i & \frac{1}{2}z_i & \frac{1}{2}r_i z_i & 0 & -\frac{1}{2}r_i z_i \\ 0 & 0 & 1 & 0 & \theta_i & -r_i & 0 & 0 & -\frac{r_i^2}{2} & -\frac{r_i^2\theta_i}{2} & 0 & 0 & -\frac{\theta_i^2}{2} & -\frac{r_i\theta_i^2}{2} & z_i & r_iz_i & \theta_i z_i & r_i\theta_i z_i & 0 & -\frac{r_i\theta_i}{2} & \frac{\theta_i}{2} & \frac{r_i\theta_i}{2} & \frac{r_i}{2} & \frac{r_i\theta_i}{2} \end{bmatrix}$$

and r_i, θ_i, z_i are the coordinates of the eight node i (i = 1, 2, 3, 4, 5, 6, 7, 8).

For an isotropic material the elasticity matrix [*D*] is written:

$$[D]=\frac{E}{(1-\nu)(1-2\nu)}\begin{bmatrix}(1-\nu) & \nu & \nu & 0 & 0 & 0\\ \nu & (1-\nu) & \nu & 0 & 0 & 0\\ \nu & \nu & (1-\nu) & 0 & 0 & 0\\ 0 & 0 & 0 & \frac{1}{2}(1-2\nu) & 0 & 0\\ 0 & 0 & 0 & 0 & \frac{1}{2}(1-2\nu) & 0\\ 0 & 0 & 0 & 0 & 0 & \frac{1}{2}(1-2\nu)\end{bmatrix}$$

REFERENCES

[1] Kim Y.H., Jones R.F., Lee S.W., 1990, Study of 20-node solid element, *Communication in Applied Numerical Methods in Engineering* **6**: 197-205.

[2] Charhabi A., 1990, Calcul des plaques minces et épaisses a` l'aide des éléments finis tridimensionnels, *Annales de l'ITBTP* **486**: 73-91.

[3] Trinh V.D., Abed-Meraim F., Combescure A., 2011, Assumed strain solid–shell formulation ''SHB6'' for the six- node prismatic, *Journal of Mechanical Science and Technology* **25**(9): 2345-2364.

[4] Ayad R., Zouari W., Meftah K., Ben Zineb T., Benjeddou A., 2013, Enrichment of linear hexahedral finite elements using rotations of a virtual spacefiber, *International Journal for Numerical Methods in Engineering* **95**(1): 46-70.

[5] Belounar L., Guerraiche K., 2014, A new strain based brick element for plate bending, *Alexandria Engineering Journal* **53**(1): 95-105.

[6] Belarbi M.T., Charif A., 1999, Développement d'un nouvel élément hexaédrique simple basé sur le modèle en déformation pour l'étude des plaques minces et épaisses, *Revue Européenne des Eléments Finis* **8**(2): 135-157.

[7] Guerraiche K., Belounar L., Bouzidi L., 2018, A new eight nodes brick finite element based on the strain approach, *Journal of Solid Mechanics* **10**(1): 186-199.

[8] Messai A., Belounar L., Merzouki T., 2019, Static and free vibration of plates with a strain based brick element, *European Journal of Computational Mechanics* **99**(1): 1-21.

[9] Dastjerdi Sh., Jabbarzadeh M., 2016, Nonlocal bending analysis of bilayer annular/circular nano plates based on first order shear deformation theory, *Journal of Solid Mechanics* **8**(3): 645-661.

[10] Dastjerdi Sh., Jabbarzadeh M., Tahani M., 2015, Nonlinear bending analysis of sector graphene sheet embedded in elastic matrix based on nonlocal continuum mechanics, *International Journal of Engineering Transactions B: Applications* **28**(5): 802-811.

[11] Dastjerdi Sh., Akgöz B., 2018, New static and dynamic analyses of macro and nano FGM plates using exact three-dimensional elasticity in thermal environment, *Composite Structures* **192**: 626-641.

[12] Belarbi M. T., Charif A., 1998, Nouvel élément secteur basé sur le modèle de déformation avec rotation dans le plan, *Revue Européenne de Eléments Finis* **7**(4): 439-458.

[13] Rebiai C., Belounar L., 2013, A new strain based rectangular finite element with drilling rotation for linear and nonlinear analysis, *Archive of Civil and Mechanical Engineering* **13**(1): 72-81.

[14] Belounar L., Guenfoud M., 2005, A new rectangular finite element based on the strain approach for plate bending, *Thin-Walled Structures* **43**(1): 47-63.

[15] Himeur M., Benmarce A., Guenfoud M., 2014, A new finite element based on the strain approach with transverse shear effect, *Structural Engineering and Mechanic* **49**(6): 793-810.

[16] Rebiai C., Belounar L., 2014, An effective quadrilateral membrane finite element for plate bending analysis, *Measurement* **50**: 263-269.

[17] Belounar A., Benmebarek S., Belounar L., 2018, Strain based triangular finite element for plate bending analysis, *Mechanics of Advanced Materials and Structures* **2018**: 1-13.

[18] Sabir A.B., Salhi H.Y.,1986, A strain based finite element for general plane elasticity in polar coordinates, *Res Mechanica* **19**(1): 1-16.

[19] Bouzriba A., Bouzerira C., 2015, Sector element for analysis of thick cylinders exposed to internal pressure and change of temperature, *Gradevinar* **67**(6): 547-555.

[20] Raju I.S., Rao A.K., 1969, Stiffness matrices for sector elements, *AIAA Journal* **7**(1): 156-157.

[21] Olson M.D., Lindberg G. M., 1970, Annular and circular sector finite element for plate bending, *IJMS* **12**: 17-33.

[22] Timoshenko S., Woinowsky-Krieger S., 1959, *Theory of Plates and Shells*, London, McGraw-Hill.

[23] Choi N., 2006, A hybrid Trefftz plane elasticity element with drilling degrees of freedom, *Computer Methods in Applied Mechanics Engineering* **195**(1): 4095-4105.

[24] Timoshenko S., Goodier J.N., 1951, *Theory of Elasticity*, McGraw-Hill New York.